Syntheses, Structures, and Spectroscopic Properties of Gold(I) Complexes of 1,3,5-Triaza-7-phosphaadamantane (TPA). Correlation of the Supramolecular Au···Au Interaction and Photoluminescence for the Species (TPA)AuCl and [(TPA-HCl)AuCl]

Zerihun Assefa, Brian G. McBurnett, Richard J. Staples, and John P. Fackler, Jr.*

Department of Chemistry and Laboratory for Molecular Structure and Bonding, Texas A&M University, College Station, Texas 77843-3255

Bernd Assmann, Klaus Angermaier, and Hubert Schmidbaur*

Anorganisch-chemisches Institut der Technischen Universität München, Lichtenbergstrasse 4, Munich D-85747, Germany

Received June 14, 1994[⊗]

The reaction of the cage-type ligand 1,3,5-triaza-7-phosphaadamantane (TPA) with (dimethyl sulfide)gold(I) chloride in a molar ratio 1:1 in aprotic polar solvents affords the complex (TPA)AuCl, **1**, in high yield. Similarly, reacting the protonated TPA ligand in $MeOH/CH_3CN$ (2:1) with (tetrahydrothiophene)AuCl gives the protonated product (TPA-HCl)AuCl, **1P**, in excellent yield. The cation of **1P** becomes deprotonated above about pH 4.5. The structures and temperature-dependent photoluminescence properties of **1** and **1P** have been determined. Protonation of the TPA ligand remarkably lengthens the solid state, auriophilic Au···Au interaction in **1P**, where the Au···Au separation is 3.322(1) Å, compared with 3.092(1) Å in **1**. The luminescence spectra of the two compounds are substantially different, clearly a consequence of the change in the Au···Au separation associated with the "supramolecular" auriophilic dimerization. While the Cl–Au–P angles are nearly linear in both compounds, 177.4 (1) and 175.8 (1)°, respectively, a "crossed" dimerization (dihedral angle P–Au–Au′–P′ about 105°) occurs. The small cone angle of the TPA ligand allows this Au···Au interaction to occur, a dimerization absent for many other tertiary phosphine complexes of LAuX which have been structurally characterized to date. At 78 K compound **1P** luminesces yellow (596 nm), while compound **1** luminesces intensely red (674 nm). The emission band of **1** is red-shifted by about 2000 cm^{-1} when compared to that of **1P**. The emission bands in both compounds blue-shift as the temperature is increased. Between 78 and 298 K the emission band of **1P** blue-shifts by about 400 cm^{-1} and that of **1** by 700 cm^{-1}. Neither complex is luminescent in solution. A solution absorption band has been observed at energies >40 000 cm^{-1} (242 nm). The interpretation of the changes in the low-energy visible emission in the solid state upon changing the auriophilic Au···Au contact is supported by extended Hückel MO calculations wherein, upon shortening the Au···Au separation, the HOMO (σ_u) orbital is destabilized, causing a decrease in the HOMO–LUMO gap. (TPA)AuCl is readily converted into the corresponding bromide, **2**, or iodide, **3**, by treating it with HBr(aq) or KI in acetone, respectively. The complex $(TPA)AuCH_3$, **4**, is obtained from (TPA)AuCl and equimolar quantities of MeLi in diethyl ether. An N-methylated complex $[(TPAMe)AuCl]OSO_2CF_3$, **5**, is formed in the reaction of (TPA)AuCl with CF_3SO_3Me in dichloromethane. Crystal data: (TPA-HCl)AuCl·0.5H_2O, **1P·0.5H_2O**, monoclinic, space group *C2/c* with a = 15.060(2) Å, b = 12.663(2) Å, c = 13.775(3) Å, β = 120.60(2)°, V = 2261.0 (6) Å^3, Z = 8, R = 0.0317 (R_w = 0.0415); (TPA)AuCl·CH_3CN, **1·CH_3CN**, orthorhombic, space group *Pbcn*, with a = 14.334(2) Å, b = 13.924(3) Å, c = 11.776(2) Å, V = 2350.3 Å^3, Z = 8, R = 0.038 (R_w = 0.0467); (TPA)AuBr·CH_3CN, **2·CH_3CN**, orthorhombic, space group *Pbcn*, a = 14.546(3) Å, b = 14.138(3) Å, c = 11.898(3) Å, V = 2431.9(9) Å, Z = 8, R = 0.544 (R_w = 0.075).

Introduction

Small cage-type ligands like the adamantane-based hexamethylenetetramine (urotropine, **A**) have very narrow cone angles[1] at their donor centers and can thus be readily accommodated even at crowded coordination centers.[2] In cases of ligand multidirectional multifunctionality—as is the case for the urotropine with its four N-donor atoms pointing along the 3-fold axes of a tetrahedron—intimately coordinated supramolecular networks can be constructed.[1,3]

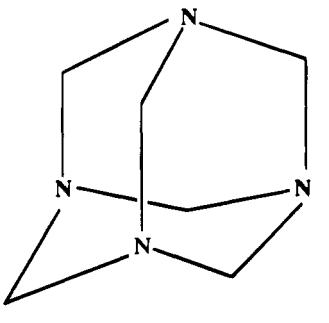

A

[⊗] Abstract published in *Advance ACS Abstracts,* November 15, 1994.

(1) (a) Pickardt, J. *Z. Naturforsch.* **1981**, *36B*, 649. (b) Pickardt, J. *Z. Naturforsch.* **1981**, *36b*, 1225.

(2) (a) Darensbourg, M. Y.; Daigle, D. *Inorg. Chem.* **1975**, *14*, 1217. (b) Delerno, J. R.; Trefonas, L. M.; Darensbourg, M. Y.; Majeste, R. J. *Inorg. Chem.* **1976**, *15*, 516.

0020-1669/95/1334-0075$09.00/0

The synthesis of the first phosphaurotropine, 1,3,5-triaza-7-phosphaadamantane (TPA, **B**),[4-6] has produced a multifunctional ligand with one donor site for the complexation of soft, low-valent, late transition elements. Its ligand chemistry has been exploited to date in only a limited number of cases.[7-9] Its behavior as a ligand for Au(I) has now been probed.

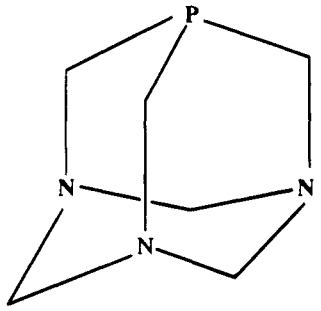

B

This study was initiated in an attempt to further delineate the general rules governing the association of Au(I) complexes through what has tentatively been addressed as the "auriophilicity" phenomenon.[10-13] In previous work[10] it could be demonstrated that, for LAuX complexes with small ligands L (neutral) and X (anionic), a pronounced aggregation through Au···Au contacts occurs which is not obscured by steric effects. Considering the small cone angle[2,7,8] of TPA (102°), it was anticipated that complex association should not be inhibited by ligand repulsion in LAuX complexes utilizing this ligand. The title compounds therefore become excellent models for the structural chemistry of crystalline Au(I) complexes.

An additional incentive for this investigation originated from the desire to prepare Au(I) complexes with *hydrophilic* tertiary phosphines, which should show unconventional solubility and reactivity patterns. An especially interesting spectroscopic observation has been made with the protonated and unprotonated title compounds which relates to the Au···Au separation in the solid materials. These compounds luminesce at a remarkably low energy in the solid state. In the absence of such close Au···Au contacts, neither the relatively low energy absorption bands nor the luminescence associated with these bands is observed.[14,15]

Photoluminescence studies of $[AuY_2]^-$ in crystalline compounds, Y = general anionic ligand, have been used to elucidate the extent of metal–metal interaction between these anions. The cyanoaurate(I) compounds have been studied extensively in this regard.[15] The $Au(CN)_2^-$ compounds of K^+, Cs^+, and Tl^+ have intermolecular Au···Au contacts[16] ranging from 3.1 to 3.64 Å, with solid state absorption bands which are red-shifted[17] by as much as 20 000 cm^{-1} from solvent-separated species. The compounds also show visible luminescence[15] which is attributed to the metal–metal interaction. When the counterions are replaced by large cations, such as NBu_4^+ and PPN^+ ($(PPh_3)_2N^+$), the intermolecular Au···Au contacts disappear[14a,18] (Au···Au separation > 8.0 Å) and the compounds are not luminescent.

With apparently few exceptions to date, the linear Au(I) complexes having a Au···Au contact < 3.6 Å are luminescent in the solid state, especially at liquid nitrogen temperature. Visible metal-centered luminescence in mononuclear Au(I) complexes appears to be associated with a trigonal, noncentrosymetric structure about the metal ion, either through intermetallic interaction or three-coordination by certain ligands.[19] Thus several three-coordinate mononuclear Au(I) complexes are now known to luminesce both in the solid state and in solution,[20] including water[21] as a solvent. Solution luminescence of Au(I) complexes otherwise is rarely observed.[20]

While an association of an auriophilic Au···Au interaction with photoluminescence appears to have been established rather generally, the influence of the ligand, L, in modifying the Au···Au interaction and the subsequent spectroscopy has been evaluated much less. A recent theoretical study by Pyykkö suggests that the Au···Au interaction in $[XAuPH_3]_2$ type complexes increases as the softness of the ligand X increases.[22] The present study demonstrates that protonation of the TPA ligand remarkably alters both the solid state auriophilic interaction and the luminescence of the complexes.

Experimental Section

General Procedures. All experiments with the unprotonated TPA ligand and its compounds were routinely carried out under pure, dry

(3) (a) Alyea, E. C.; Fischer, K. J.; Johnson, S. *Can. J. Chem.* **1989**, *67*, 1319. (b) Fischer, K. J.; Alyea, E. C.; Shahnazarian, N. *Phosphorus, Sulfur Silicon* **1990**, *48*, 37.
(4) Daigle, D. J.; Pepperman, A. B.; Vial, S. L. *J. Heterocycl. Chem.* **1974**, *11*, 407.
(5) Daigle, D. J.; Pepperman, A. B. *J. Heterocycl. Chem.* **1975**, *12*, 579.
(6) Fluck, E.; Förster, J. E.; Weidlein, J.; Hädicke, E. *Z. Naturforsch.* **1977**, *32B*, 499.
(7) De Lerno, J. R.; Trefonas, L. M.; Darensbourg, M. Y.; Majeste, R. J. *Inorg. Chem.* **1976**, *15*, 816.
(8) Darensbourg, D. Y.; Joo, F.; Kannisto, M.; Katho, A.; Reibenspies, J. H. *Organometallics* **1992**, *11*, 1990.
(9) Alyea, E. C.; Fischer, K. J.; Johnson, S. *Can. J. Chem.* **1989**, *67*, 1319.
(10) Schmidbaur, H. *Gold Bull.* **1990**, *23*, 11–21.
(11) Pyykkö, P. *Chem. Rev.* **1988**, *88*, 563.
(12) (a) Rösch, N.; Görling, A.; Ellis, D. E.; Schmidbaur, H. *Angew. Chem., Int. Ed. Engl.* **1989**, *28*, 1357; *Angew. Chem.* **1989**, *101*, 1410. (b) Görling, A.; Rösch, N.; Ellis, D. E.; Schmidbaur, H. *Inorg. Chem.* **1991**, *30*, 3986.
(13) (a) Jones, P. G. *Gold Bull.* **1981**, *14*, 102–118, 159–166; **1983**, *16*, 114–124; **1986**, *19*, 46–57. (b) Uson, R.; Laguna, A. *Coord. Chem. Rev.* **1986**, *70*, 1. (c) Khan, M. N. I.; King, C.; Heinrich, D. D.; Fackler, J. P., Jr.; Porter, L. C. *Inorg. Chem.* **1989**, *28*, 2150. (d) Khan, M. N. I.; Fackler, J. P., Jr.; King, C.; Wang, J. C.; Wang, S. *Inorg. Chem.* **1988**, *27*, 1672. (e) Schmidbaur, H.; Graf, W.; Muller, G. *Angew. Chem., Int. Ed. Engl.* **1988**, *23*. (f) Khan, M. N. I.; Wang, S.; Fackler, J. P., Jr. *Inorg. Chem.* **1989**, *28*, 3588. (g) Vogler, A.; Kunkeley, H. *Chem. Phys. Lett.* **1988**, *150*, 135. (h) Schmidbaur, H.; Dziwok, K.; Grohmann, A.; Müller, G. *Chem. Ber.* **1989**, *122*, 893. (i) Schmidbaur, H.; Lachmann, J.; Wilkinson, D. L.; Müller, G. *Chem. Ber.* **1990**, *123*, 423. (j) Narayanaswamy, R.; Young, M. A.; Parkhurst, E.; Quellette, M.; Kerr, M. E.; Ho, D. M.; Elder, R. C.; Bruce, A. E.; Bruce, M. R. M. *Inorg. Chem.* **1993**, *32*, 2506.
(14) (a) Mason, W. R. *J. Am. Chem. Soc.* **1976**, *98*, 5182. (b) Chastain, S. K.; Mason, W. R. *Inorg. Chem.* **1982**, *21*, 3717. (c) Bowmaker, G. A.; Boyd, P. D.; Sorrenson, R. J. *J. Chem. Soc., Faraday, Trans. 2* **1985**, *81*, 1627. (d) Savas, M .M.; Mason, W. R. *Inorg. Chem.* **1987**, *26*, 301.
(15) (a) Patterson, H. H.; Roper, G.; Biscoe, J.; Ludi, A.; Blom, N. *J. Lumin.* **1984**, *31/32*, 555. (b) Assefa, Z.; DeStefano, F.; Garepapaghi, M.; LaCasce, J., Jr.; Ouellete, S.; Corson, M.; Nagle, J.; Patterson, H. H. *Inorg. Chem.* **1991**, *30*, 2868. (c) Assefa, Z.; Shankle, G.; Patterson, H. H.; Reynolds, R. *Inorg. Chem.* **1994**, *33*, 2187. (d) Nagle, J.; LaCasce, J., Jr.; Corson, M.; Dolan, P. J., Jr.; Assefa, Z.; Patterson, H. H. *Mol. Cryst. Liq. Cryst.* **1990**, *181*, 356. (e) Markert, J. T.; Blom, N.; Roper, G.; Perregaux, A. D.; Nagasundaram, N.; Corson, M. R.; Ludi, A.; Nagle, J. K.; Patterson, H. H. *Chem. Phys. Lett.* **1985**, *118*, 258. (f) Nagasundaram, N.; Roper, G.; Biscoe, J.; Chai, J. W.; Patterson, H. H.; Blom, N.; Ludi, A. *Inorg. Chem.* **1986**, *25*, 2947.
(16) (a) Rosenzweig, A.; Cromer, D. *Acta Crystallogr.* **1959**, *12*, 709. (b) Blom, N.; Ludi, A.; Burgi, H.-B.; Tichy, K. *Acta Crystallogr., Sect. C.: Cryst. Struct. Commun.* **1984**, *C40*, 1767.
(17) Blum, N. Thesis, University of Berne, 1983.
(18) Assefa, Z.; Staples, R. J.; Fackler, J. P., Jr., *Acta Crystallogr.*, submitted for publication.
(19) (a) McClesky, T.; Gray, H. B. *Inorg. Chem.* **1992**, *31*, 1733. (b) King, C.; Wang, J.-C.; Khan, M. N. I.; Fackler, J. P., Jr. *Inorg. Chem.* **1989**, *28*, 2145. (c) Yam, V. W.-W.; Lee, W.-K. *J. Chem. Soc., Dalton Trans.* **1993**, 2097.
(20) King, C.; Khan, M. N. I.; Staples, R. J.; Fackler, J. P., Jr. *Inorg. Chem.* **1992**, *31*, 3236.
(21) Assefa, Z.; Forward, J. M.; Fackler, J. P., Jr. In preparation.
(22) Pyykkö, P.; Li, J.; Runeberg, N. *Chem. Phys. Lett.* **1994**, *218*, 133.

nitrogen. Solvents were purified prior to use or were spectral grade (acetonitrile). Water was deionized and doubly distilled. Glassware was oven-dried and filled with nitrogen. Instruments: NMR, JEOL JNM GX 400 and 270 and a Bruker 250; MS, Varian MAT 90; UV–vis spectra, Cary Models 14 and 17; thermal analysis, IA9200, Electrothermal ENG. Ltd.; emission and excitation spectra, SLM AMINCO, Model 8100 spectrofluorimeter using a xenon lamp. Spectra are corrected for instrumental response. The radiation was filtered through a 0.10 M KNO_2 solution to reduce the amount of scattered light. Low-temperature measurements were made in a cryogenic device of local design. Crycon grease and collodion were used to attach the crystal and powder samples, respectively, to the holder. The grease and collodion were scanned for baseline subtraction. Acetone/dry ice (200 K) and CCl_4/N_2 (250 K) baths were used to control the temperature above 78 K. The following reagents were prepared by following literature procedures: TPA, ref 5; $(Me_2S)AuCl$, ref 23; (tht)AuCl, ref 24. All other reagents were commercially available.

Synthesis of the 1,3,5-Triaza-7-phosphaadamantane (TPA) Ligand. The TPA ligand was prepared by following literature procedures.[3b,5] Depending on the initial pH of tetrakis(hydroxymethyl)phosphonium chloride, both the protonated and the unprotonated derivatives of the ligand are obtained. Titrating the tetrakis(hydroxymethyl)phosphonium chloride to a pH < 6.5 provided the protonated, (TPAH)Cl, ligand whereas at a pH ca. 8 or greater the unprotonated product TPA was obtained. Recrystallization from MeOH solution provided the pure product. The protonated [TPAH]Cl ligand in D_2O gave a $^{31}P\{^1H\}$ resonance at −89.5 ppm (s) while unprotonated TPA shows a $^{31}P\{^1H\}$ NMR signal at −96.7 ppm (s).[3b]

Synthesis of (1,3,5-Triaza-7-phosphaadamantane-*P*)gold(I) Chloride, (TPA)AuCl, 1. A solution of TPA (233 mg, 1.48 mmol) in chloroform (25 mL) is added at room temperature, slowly with stirring, to a solution of $(Me_2S)AuCl$ (436 mg, 1.48 mmol) in $CHCl_3$ (20 mL). After 2 h the precipitate is collected and washed with small portions of $CHCl_3$: yield 550 mg (95%); dec 223 °C without melting. Anal. Calcd for $C_6H_{12}AuClPN_3$ (fw 389.57): C, 18.49; H, 3.12; N, 10.79. Found: C, 18.69; H, 3.14; N, 10.76. ^1H NMR (DMSO-d_6): δ 4.35 [d, J(P,H) = 9.8 Hz, PCH_2], 4.53 [s, NCH_2N_{ax}], 4.48 [s, NCH_2N_{eq}]. $^{13}C\{^1H\}$ NMR (DMSO-d_6): δ 71.82 [d, J(P,C) = 8.3 Hz, NCN], 50.93 [d, J(P,C) = 23.1 Hz, PCN]. $^{31}P\{^1H\}$ NMR: δ −51.4 (s). MS(FD): m/z = 389 (100%) [M^+].

The crystalline solvated materials, **1·CH$_3$CN** and **2·CH$_3$CN** (see below), are obtained by crystallization from methylene chloride/acetonitrile. Compound **1** also can be synthesized as for **1P** (below) by using the unprotonated TPA ligand. Alternatively **1·CH$_3$CN** can be obtained by deprotonation of **1P** with 0.1 N NaOH and crystallization from methylene chloride/acetonitrile. Similarly, dissolving **1** in 0.1 N HCl and slowly evaporating the solvent provides single crystals of **1P·0.5H$_2$O**. (Preliminary work[21] at Texas A&M has established that the pK_a for deprotonation of the various protonated (TPA)AuCl complexes in water is about 4.5.) The luminescence study was conducted on these crystals.

Synthesis of (1,3,5-Triaza-7-phosphaadamantane-*P* hydrochloride)gold(I) Chloride, [(TPA-HCl)AuCl]·0.5H$_2$O, 1P·0.5H$_2$O. To a stirred suspension of (tht)AuCl (182.8 mg, 0.57 mmol) in 10 mL of MeOH/CH_3CN (2:1) is added the protonated TPA ligand (110 mg, 0.57 mmol) in one portion. In about 5 min a gelatinous sticky precipitate appears which turns to a fine precipitate in ca. 15 min. After 2 h of further stirring, 5 mL of Et_2O is added to precipitate the entire product. The precipitate is filtered off, washed with cold EtOH (1 mL × 2) and Et_2O, and dried under vacuum to afford 206 mg of product (93% yield). $^{31}P\{^1H\}$ NMR (D_2O/H_2O, 1:10, reference H_3PO_4): δ −38.9 (s). $^{13}C\{^1H\}$ NMR (D_2O): δ −49.5 [d, J(P,C) = 19 Hz], −71.1 (s). ^1H (D_2O) NMR signals are masked by H_2O signals.

Synthesis of (1,3,5-Triaza-7-phosphaadamantane-*P*)gold(I) Bromide, (TPA)AuBr, 2. Aqueous HBr (47% w/w, 2 mL) is added to a boiling solution of complex **1** (138 mg, 0.35 mmol) in acetone (60 mL). After 90 min at reflux and slow cooling to ambient temperature, the orange-brown reaction mixture is filtered and the solid product recrystallized from acetonitrile: yield 70 mg (47%); colorless flaky powder, soluble in DMSO and DMF and slightly soluble in CH_3CN. ^1H NMR (DMSO-d_6): δ 4.33 [d, J(P,H) = 9.0 Hz, 6H, PCH_2N], 4.54 and 4.49 [each s, 3H, NCH_2N]. $^{13}C\{^1H\}$ NMR: δ 70.57 [d, J(P,C) = 6.6 Hz, NCN], 48.47 [d, J(P,C) = 23.4 Hz, PCN]. $^{31}P\{^1H\}$ NMR: δ −47.3 (s).

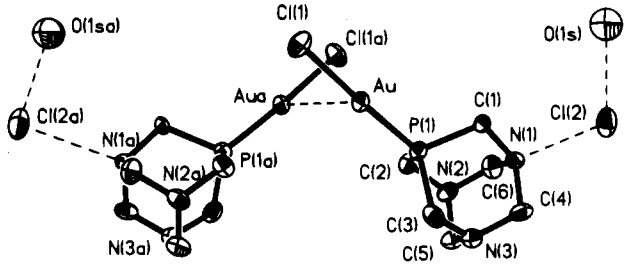

Figure 1. Thermal ellipsoid drawing of **1P·0.5H$_2$O** in 50% probability.

Synthesis of (1,3,5-Triaza-7-phosphaadamantane-*P*)gold(I) Iodide, (TPA)AuI, 3. A suspension of complex **1** (100 mg, 0.26 mmol) in boiling acetone (50 mL) is treated with a slurry of KI (128 mg, 0.77 mmol) in acetone (50 mL). After 1 h at reflux temperature and overnight stirring at ambient temperature, the solvent is removed in a vacuum and the residue extracted with boiling acetonitrile. The product precipitates from the solvent on cooling: yield 80 mg (64%); colorless needles; mp 244 °C dec. Anal. Calcd for $C_6H_{12}AuIPN_3$ (fw 481.03): C, 14.97; H, 2.49; N, 8.73. Found: C, 14.50; H, 2.47; N, 8.21. ^1H NMR (DMSO-d_6): δ 4.33 [d, J(P,H) = 9.0 Hz, 6H, PCH_2N], 4.54 and 4.49 [each s, 3H, NCH_2N]. $^{31}P\{^1H\}$ NMR: δ −47.6 (s). MS(FD): m/z = 481 (100%) [M^+].

Synthesis of Methyl(1,3,5-triaza-7-phosphaadamantane-*P*)gold(I), (TPA)AuCH$_3$, 4. Complex **1** (146 mg, 0.37 mmol) dispersed in diethyl ether (20 mL) is treated at 0 °C with a solution of methyllithium (2 mL, 0.5% (w/w), 0.4 mmol) in Et_2O. After overnight stirring, the solvent is removed in a vacuum and the residue extracted with CH_2Cl_2: yield 65 mg (47%); colorless powder; mp 143 °C dec. ^1H NMR (DMSO-d_6): δ 0.09 [d, J(P,H) = 7.8 Hz, 3 H, AuMe], 4.31 [d, J(P,H) = 9.8 Hz, 6H, PCH_2N], 4.53 and 4.48 [each s, 3H, NCH_2N]. $^{13}C\{^1H\}$ NMR: δ 71.98 [d, J(P,C) = 7.2 Hz, NCN], 50.98 [d, J(P,C) = 14.9, PCN], 9.72 [d, J(P,C) = 94.8 Hz, AuMe]. $^{31}P\{^1H\}$ NMR: δ −36.6 (s).

Synthesis of Chloro(1-methyl-1,3,5-triaza-7-phosphaadamantanium-*P*)gold(I)(1+) Trifluoromethanesulfonate(1−), [(MeTPA)-AuCl]SO$_3$CF$_3$, 5. A slurry of complex **1** (150 mg, 0.38 mmol) in CH_2Cl_2 (10 mL) is treated at −35 °C with $MeOSO_2CF_3$ (0.06 mL, 0.55 mmol). The mixture is allowed to warm to ambient temperature over a period of 4 h. The solvent and other volatiles are removed in a vacuum, and the residue is crystallized from hot acetone: yield 181 mg (85%); colorless solid; mp 124 °C. Anal. Calcd for $C_8H_{15}AuClF_3N_3O_3PS$ (fw 553.68): C, 17.34; H, 2.71; N, 7.59. Found: C, 18.14; H, 2.88; N, 7.33. ^1H NMR (DMSO-d_6): δ 2.73 [d, J(P,H) = 2.1 Hz, 3H, NMe], 4.1–5.1 [m, 12H, CH_2]. $^{13}C\{^1H\}$ NMR: δ 79.8 [d, J(P,C) = 5.0 Hz, NCN^+], 68.39 [d, J(P,C) = 7.2 Hz, NCN], 55.65 [d, J(P,C) = 24.8 Hz, PCN^+], 48.95 [s, NMe^+], 23.68 [d, J(P,C) = 23.7 Hz, PCN]. $^{31}P\{^1H\}$ NMR: δ −33.1 (s). MS(FAB): m/z = 404 (41.4%) [(**5** − CF_3SO_3)$^+$], 518 (3.2%) [(**5** − Cl)$^+$]; 361 (7.6%) [M^+ − (CH_2=NMe)]; 172 (100%) [$TPAMe^+$].

Structural Data. The structure of **1P·0.5H$_2$O** was determined at College Station on data collected at room temperature on a Nicolet R3m/E diffractometer (SHELXTL 5.1) by employing monochromated Mo Kα radiation (λ 0.710 73 Å). A colorless needle 0.5 × 0.2 × 0.1 mm^3 was mounted on a glass filter with epoxy cement at room temperature. The unit cell constants were determined from 25 machine-centered reflections. Intensities of all reflections with 2θ values 4–45 °C were measured by ω-scanning technique. Lorentz and polarization corrections were applied. Empirical absorption corrections based on azimuthal (ψ) scans of reflections were made. The structure was solved using direct methods, SHELXTL 5.1, with difference Fourier syntheses giving the missing non-hydrogen atoms. See Table 1 for crystallographic data. Figure 1 is a thermal ellipsoid drawing of the structure, and Table 2 contains atom coordinates. Selected bond distances and

(23) Dash, K. C.; Schmidbaur, H. *Chem. Ber.* **1973**, *106*, 1221.
(24) Uson, R.; Laguna, A.; Vicente, J. *J. Chem. Soc., Chem. Commun.* **1976**, 353.

Table 1. Crystallographic Data for **1P·0.5H$_2$O**, **1·CH$_3$CN**, and **2·CH$_3$CN**

	1P·0.5H$_2$O	**1·CH$_3$CN**	**2·CH$_3$CN**
formula	$C_6H_{14}N_3O_{0.5}PCl_2Au$	$C_8H_{15}N_4PClAu$	$C_8H_{15}N_4PBrAu$
fw	435.04	430.63	475.08
space group	*C*2/*c* (no. 15)	*Pbcn* (No. 60)	*Pbcn* (No. 60)
a, Å	15.060(2)	14.334(2)	14.546(3)
b, Å	12.663(2)	13.924(3)	14.138(3)
c, Å	13.775(2)	11.776(2)	11.898(3)
α, deg	90.00	90.00	90.00
β, deg	120.60(2)	90.00	90.00
γ, deg	90.00	90.00	90.00
V, Å^3	2261.0(6)	2350.3	2431.9(9)
Z	8	8	8
d_{calc}, g/cm^3	2.56	2.43	2.58
μ(Mo Kα), mm^{-1}	13.58	12.86	15.44
λ (Mo Kα), Å	0.710 73	0.710 69	0.710 73
temp, K	293	193	293
transm factor: max, min	0.953	0.999	0.910
	0.747	0.696	0.532
R,[a] R_w[b]	0.0317, 0.0415	0.0380, 0.0467	0.0544, 0.0750

[a] $R = \sum||F_o| - |F_c||/\sum|F_o|$. [b] $R_w = [\sum w(|F_o| - |F_c|)/\sum w|F_o|]^{1/2}$; $w^{-1} = [\sigma^2(|F_o|) = g|F_o|^2]$.

Table 2. Atomic Coordinates (×10^4) and Equivalent Isotropic Displacement Parameters (Å^2 × 10^3) for (TPA-HCl)AuCl·0.5H$_2$O, **1P·0.5H$_2$O**

	x	*y*	*z*	*U*(eq)[a,b]
Au	9707(1)	242(1)	8510(1)	27(1)
Cl(1)	11103(2)	−865(2)	9386(2)	38(1)
Cl(2)	4041(2)	655(3)	5854(2)	50(1)
P(1)	8308(2)	1251(2)	7648(2)	25(1)
N(1)	6245(5)	1462(6)	6907(6)	26(3)
N(2)	6844(6)	2190(6)	5700(6)	29(3)
N(3)	7288(6)	3077(6)	7470(6)	28(4)
C(1)	7140(6)	688(8)	7535(8)	26(4)
C(2)	7785(7)	1540(8)	6154(7)	29(4)
C(3)	8299(7)	2582(8)	8194(8)	32(4)
C(4)	6459(8)	2527(8)	7511(8)	31(4)
C(5)	7038(8)	3193(8)	6298(8)	34(5)
C(6)	6027(7)	1631(8)	5704(7)	33(4)
O(1S)	5000	1310(11)	2500	88(9)

[a] Equivalent isotropic *U* defined as one-third of the trace of the orthogonalized U_{ij} tensor. [b] Estimated standard deviations are given in parentheses.

Table 3. Selected Distances (Å) and Angles (deg)

	1P·0.5H$_2$O (X = Cl)	**1·CH$_3$CN** (X = Cl)	**2·CH$_3$CN** (X = Br)
Au−X	2.294(3)	2.304(2)	2.379(4)
Au−P	2.221(2)	2.226(2)	2.227(6)
Au−Au	3.322(1)	3.092(1)	3.107(2)
X−Au−P	177.4(1)	175.8(1)	175.7(2)
X−Au−Au	82.9(1)	90.5(1)	92.1(1)
P−Au−Au	97.8(1)	93.6(1)	92.0(2)

[a] Estimated standard deviations are given in parentheses.

angles for each compound studied crystallographically are given in Table 3.

The structure of **1·CH$_3$CN** was determined at Garching on data collected with a CAD4 diffractometer using monochromated Mo Kα (λ 0.710 69 Å) radiation, from a small crystal held at −80 °C. An empirical absorption correction was applied after Lorentz and polarization corrections to the data obtained. The structure solution was done by direct methods, with all missing non-hydrogen atoms located by successive difference Fourier syntheses. See Table 1 for crystallographic data. Figure 2 is a thermal ellipsoid drawing of the structure, and Table 4 contains atom coordinates.

The structure of **2·CH$_3$CN** was completed at College Station as for **1P·0.5H$_2$O**, Figure 3. Crystallographic data are in Table 1, and atom coordinates are found in Table 5, with selected bond distances and angles in Table 3.

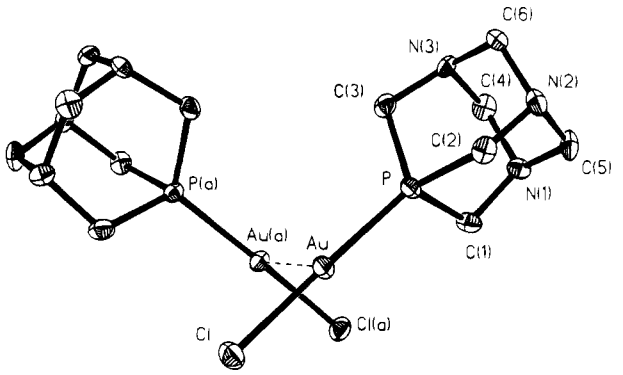

Figure 2. Thermal ellipsoid drawing of **1·CH$_3$CN** in 50% probability.

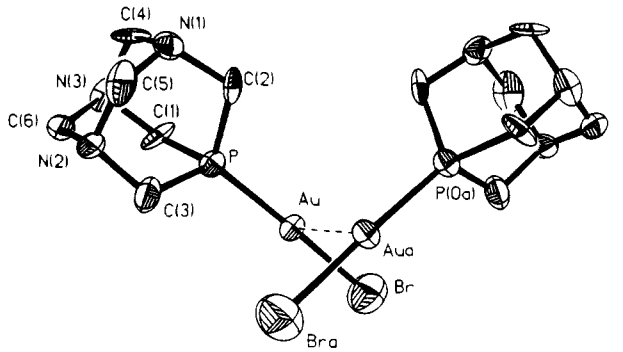

Figure 3. Thermal ellipsoid drawing of **2·CH$_3$CN** in 50% probability.

Table 4. Fractional Atomic Coordinates and Equivalent Isotropic displacement Parameters for **1·CH$_3$CN**

atom	*x*/*a*	*y*/*b*	*z*/*c*	*U*(eq), Å^2
Au	0.05828(2)	0.05399(2)	0.13952(2)	0.017
P	0.1624(1)	−0.0438(1)	0.2190(2)	0.016
Cl	−0.0416(1)	0.1573(1)	0.0469(2)	0.024
N(1)	0.2975(4)	−0.0686(4)	0.3803(5)	0.019
N(2)	0.3216(4)	−0.1495(4)	0.1942(5)	0.020
N(3)	0.2043(4)	−0.2109(4)	0.3313(6)	0.022
N(4)	0.6020(5)	−0.1211(6)	−0.1476(6)	0.035
C(1)	0.2310(5)	0.0035(5)	0.3395(6)	0.020
C(2)	0.2582(5)	−0.0882(5)	0.1295(5)	0.018
C(3)	0.1251(5)	−0.1563(5)	0.2827(6)	0.020
C(4)	0.2507(5)	−0.1575(5)	0.4184(5)	0.022
C(5)	0.3631(4)	−0.0965(6)	0.2878(6)	0.023
C(6)	0.2732(4)	−0.2359(5)	0.2390(7)	0.021
C(7)	0.4379(4)	−0.1218(6)	−0.0452(7)	0.024
C(8)	0.5289(5)	−0.1212(5)	−0.1017(6)	0.019

Molecular Orbital (MO) Calculations. Extended Hückel (EH) MO calculations were performed on a Macintosh IIfx computer using the molecular modeling CAChe software package.[25] Energy minimization was conducted using the MM2 program, which is included in the CAChe software, prior to running the EH calculation. The orbital energy and exponent parameters used in the EH calculation were obtained from Pyykkö's work and correspond to relativistic values.[26] For p and d orbitals the weighted averages of the low and high angular momentum values were used to satisfy the CAChe criteria (Table 6). For the two-coordinate complexes in $C_{\infty v}$ and $D_{\infty h}$ symmetries, the *z* axis is taken as the molecular axis. For the dimers, the Au···Au vector is taken as the *z* axis.

(25) CAChe (Computer Aided Chemistry), CAChe Scientific, Inc., TEKTRONIX Co., Beaverton, OR 97077.

(26) (a) Pyykkö, P. *Chem. Rev.* **1988**, *88*, 563. (b) Pyykkö, P. *Methods In Computational Chemistry*; Wilson, S., Ed.; Plenum Press: New York, 1988; Vol. 2, pp 137−221. (c) Pyykkö, P.; Lohr, L. L. *Inorg. Chem.* **1981**, *20*, 1950. (d) Mehrotra, P.; Hoffmann, R. *Inorg. Chem.* **1978**, *17*, 2187. (e) Jiang, Y.; Alvarez, S.; Hoffmann, R. *Inorg. Chem.* **1985**, *24*, 749. (f) Pyykkö, P.; Desclaux, J.-P. *Acc. Chem. Res.* **1979**, *12*, 276.

Table 5. Atomic Coordinates ($\times 10^4$) and Equivalent Isotropic Displacement Parameters ($Å^2 \times 10^3$) for (TPA)AuBr·CH_3CN, **2·CH_3CN**

	x	y	z	U(eq)[a,b]
Au	599(1)	517(1)	1419(1)	31(1)
Br	−416(2)	1578(3)	488(3)	79(2)
P	1628(4)	−452(4)	2191(5)	29(2)
N(1)	2038(14)	−2113(14)	3274(17)	37(8)
N(2)	2972(14)	−707(13)	3782(17)	38(8)
N(3)	3210(13)	−1496(15)	1959(15)	34(7)
C(1)	2563(18)	−888(18)	1304(20)	40(9)
C(2)	1250(14)	−1566(17)	2818(20)	34(9)
C(3)	2310(15)	−17(21)	3346(22)	44(10)
C(4)	2725(17)	−2338(15)	2400(20)	35(9)
C(5)	2485(18)	−1546(21)	4160(21)	51(11)
C(6)	3614(17)	−985(17)	2852(23)	39(10)
N(1S)	4046(17)	1188(17)	1448(20)	52(9)
C(1S)	5624(19)	1214(24)	464(24)	61(12)
C(2S)	4695(18)	1188(18)	1036(20)	32(9)

[a] Equivalent isotropic U defined as one-third of the trace of the orthogonalized U_{ij} tensor. [b] Estimated standard deviations are given in parentheses.

Table 6. Extended Hückel Relativistic Parameters[a] Obtained from Ref 26c

	orbital	$-H_{ij}$	slater exponent
Au	6s	7.94 (9.23)	2.12 (1.76)
	6p	3.47 (3.52)	1.50 (1.36)
	5d	12.37 (11.8)	3.47 (3.56)
P	3s	19.3 (16.15)	1.82 (1.82)
	3p	9.52 (10.49)	1.48 (1.48)
	3d	2.11 (2.110)	1.73 (1.73)
Cl	3s	29.38 (24.54)	2.26 (2.25)
	3p	13.76 (12.97)	1.90 (1.90)
C	2s	19.36 (16.59)	1.58 (1.58)
	2p	11.03 (11.26)	1.43 (1.45)
N	2s	26.25 (20.33)	1.87 (1.88)
	2p	13.83 (14.53)	1.73 (1.73)
H	1s	13.61 (13.61)	1.0 (1.2)

[a] Data in parentheses are default parameters included in the CAChe system.

Results

Preparative Studies. The reaction of equimolar quantities of TPA and (Me_2S)AuCl in chloroform at ambient temperature gives almost quantitative yields of (TPA)AuCl, **1**, as a colorless crystalline product, which decomposes at 223 °C without melting. It is soluble in aprotic polar solvents like dimethyl sulfoxide, acetonitrile, or dimethylformamide. In the field desorption mass spectrum, only the molecular ion is observed, $m/z = 389$ (100%) [M^+]. The composition has been confirmed by elemental analysis. The ^1H NMR spectrum of **1** in DMSO shows the same signal multiplicity as the spectrum of the free TPA ligand, suggesting that the 3-fold symmetry is retained. There are considerable shift differences for all atoms, however, the largest being associated with the phosphorus atom, consistent with the formation of a P-bonded AuCl complex of C_3 symmetry in solution.

The protonated complex (TPA-HCl)AuCl·0.5H_2O, **1P·0.5H_2O**, can be obtained from the protonated ligand or from the unprotonated Au(I) complex in aqueous HCl. As for the unprotonated species, the largest change in the NMR spectrum between the protonated ligand and the protonated complex is observed with $\delta(^{31}P)$. The rapid proton/deuterium exchange in D_2O/H_2O (1:10), however, precludes identification by ^1H NMR of the reduced ligand symmetry which must result from protonation at one N atom.

Treatment of the chloride complex **1** with a solution of excess aqueous hydrogen bromide (47%) in boiling acetone gives a ca. 50% yield of the bromide complex (TPA)AuBr (**2**), which is difficult to purify. However the crystalline product **2·CH_3CN** was obtained as described. The corresponding iodide (TPA)AuI, **3**, is obtained from the reaction of complex **1** with excess KI in boiling acetone. It can be crystallized from acetonitrile as colorless needles, which melt with decomposition at 244 °C. The solubility properties and spectral data are similar to those of **1** and **2**.

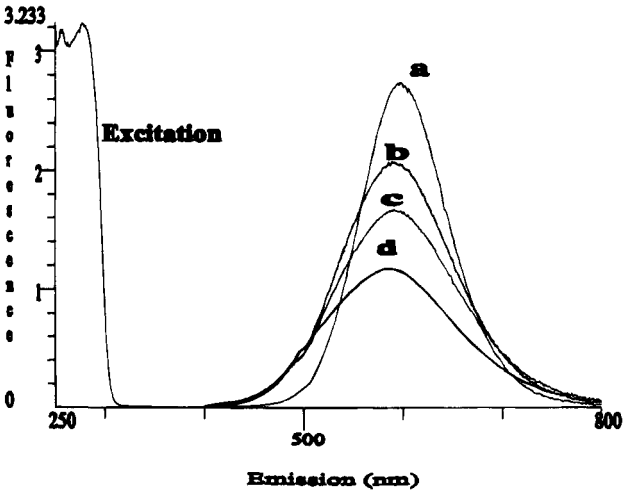

Figure 4. Temperature-dependent emission spectra of **1P**: (a) 78 K; (b) 200 K; (c) 250 K; (d) 298 K. The excitation spectrum was recorded at 78 K.

Complex **1** can be converted into the methylgold complex **4**, through the reaction with equimolar quantities of methyllithium as a *nucleophile* in diethyl ether at 0 °C. The yield of this product is only ca. 50% owing to the limited thermal stability in solution. The colorless crystalline solid decomposes at 143 °C. It is readily identified as a C_3-symmetry P−Au−CH_3 complex by its spectral data (see Experimental Section).

The *electrophilic* methylating agent $MeOSO_2CF_3$ transforms complex **1** into a singly N-methylated ammonium triflate $[(TPAMe)AuCl]^+OSO_2CF_3^-$, **5**, in high yields (85%); mp 124 °C. The product can be crystallized from boiling acetone. It is soluble in DMSO, DMF, methanol, acetonitrile, and chloroform. The composition drawn in the formula is derived from elemental analysis and *f*ast *a*tom *b*ombardment *m*ass *s*pectral data, FAB-MS. N-Methylation is suggested by the NMR data, which indicate the lowering of the ligand symmetry to point group C_s. N-Methylation of TPA also has been observed for the free ligand with methyl iodide,[16] and the spectral data show conclusive parallels for the products of the two reactions.

Luminescence Studies. Both **1** and **1P** are luminescent in the solid state. Figure 4 presents the temperature-dependent emission and excitation spectra of microcrystalline samples of **1P**. At 78 K, compound **1P** displays a strong yellow emission at 596 nm (16 780 cm^{-1}) when excited at 290 nm. The emission maximum slightly blue shifts as the temperature is increased. Between 78 and 298 K, the band maximum blue-shifts by about 400 cm^{-1}. At 200 K, the temperature at which some structural comparisons are made, the emission maximum is at 17 000 cm^{-1}. Compound **1** shows an intense red emission at low temperatures. In Figure 5, the temperature-dependent emission spectra of **1** are shown. When compared to that of **1P**, the emission band of **1** is red-shifted by about 2000 cm^{-1}. At 78 K, the emission maximum of **1** is observed at 674 nm (14 836 cm^{-1}). With an increase in the temperature, the emission intensity of **1** also decreases and the band maximum blue-shifts. At 200 K, the emission intensity is reduced by about 50% and the band is blue-shifted by about 400 cm^{-1} to 15 244 cm^{-1}. At

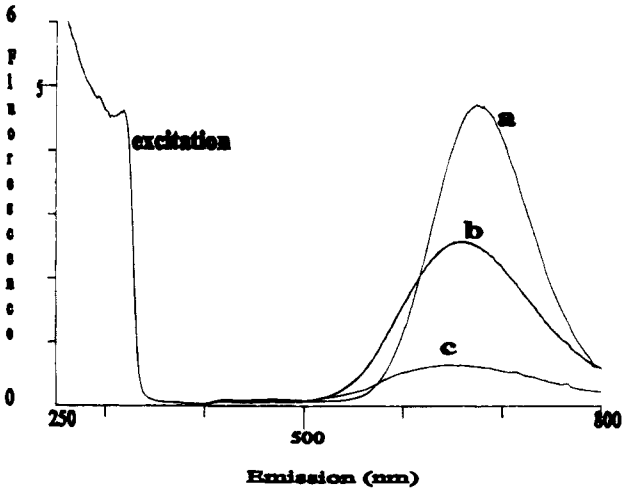

Figure 5. Temperature-dependent emission spectra of **1**: (a) 78 K; (b) 200 K; (c) 250 K. Emission is quenched at room temperature. The excitation spectrum was recorded at 78 K.

250 K, the band blue-shifts further (by about 700 cm^{-1} when compared with the 78 K spectrum) and is observed at 645 nm. The intensity is also drastically reduced. The room-temperature emission is nearly quenched. Neither complex is luminescent in solution or in a dilute ($<10^{-5}$ M) MeOH glass.

Solution absorption spectra of **1P** and **1** in CH_3CN are nearly identical (not shown). In the 220–400 nm range two bands are observed, 228 and 242 nm, for both **1P** and **1** with extinction coefficients of approximately 6×10^3 M^{-1} cm^{-1}.

Structural Observations. All analytical and spectroscopic data for **1** and **1P** in the *solution state* in strongly polar solvents suggest that the complexes are monomers with a 3-fold axial symmetry. However, these results do not eliminate association of the monomers in the solid state since it has been demonstrated that aggregation of Au(I) complexes, LAuX, through weak intermolecular Au···Au contacts may only become apparent in the condensed phase. Bond energies associated with these second-order interactions between closed-shell (d^{10}) Au(I) atoms ("auriophilicity") are only of the order of 5–10 kcal/mol, as determined[13e] in a number of experiments[13i,j] and confirmed by theoretical studies,[22] and, thus, are easily overcome by solvation of the individual components. The small cone angle of the TPA ligand (102°) suggests minimal steric hindrance for the mutual approach of the Au(I) centers of a pair or larger grouping of the (TPA)AuCl or protonated [(TPAH)AuCl]Cl complexes, and aggregation therefore was to be expected in the solid state. This hypothesis was tested by crystal structure determinations on single crystals of **1**, **1P**, and **2**.

Compounds **1** and **2** crystallize from acetonitrile with 1 equiv of solvent per Au(I) complex, while **1P** crystallizes from aqueous MeOH/CH_2Cl_2 with 0.5 mol of water. The water appears at a 2-fold symmetry position in the crystalline lattice, while there is no imposed crystallographic symmetry in **1**. Compound **2** crystallizes in an orthorhombic space group. The individual molecules of each structure have a crossed "torch" or "lollypop" molecular structure, Figures 1 and 2, with a nearly linear Cl–Au–P "handle" and nearly identical Au–Cl distances, 2.294(3) Å in **1P** and 2.304(2) Å in **1**. The Au–Br distance in **2** is 2.379 Å. The Au–P distances are 2.221(2) and 2.226(2) Å, respectively, for the protonated and unprotonated complexes (**1P** and **1**) and 2.227(4) Å in the bromide complex, **2**. The C–N distance in the protonated complex, 1.53(1) Å, is longer than the longest C–N distance, 1.509(9) Å, in the unprotonated complexes. The dimensions and conformation of the TPA ligand are very similar in the free TPA ligand to those of TPA in the coordinated species.

The critical difference between the protonated and unprotonated species is observed in the Au···Au distances. Complexes **1**, **1P**, and **2** are dimers of approximately C_2 symmetry in the crystal, with the closest approach occurring between the two Au atoms. In the unprotonated chloride species, **1**, at −80 °C, this distance is 3.092(1) Å, while the distance lengthens to 3.322(1) Å in the protonated species, **1P**, at 298 K. It is 3.104(2) Å in the unprotonated bromide complex, **2**, at 298 K. The Au···Au distance in **1P·0.5H₂O** shrinks to 3.304 Å at −80 °C as determined by the cell constant changes observed at this temperature. For **2·CH₃CN** at −80 °C, cell constant changes indicate the Au···Au distance to be 3.089 Å.

Discussion

The type of atom arrangements observed for both the protonated and unprotonated complexes reported here are typical of L–Au–X species and corroborate some pertinent theoretical predictions based on the auriophilicity concept. Pyykkö recently suggested[22] that, for two-coordinate $[XAuPH_3]_2$ compounds, the relativistic auriophilic attraction is directly correlated with the softness of the ligand X. Since X is chloride in two of the complexes reported here, it is interesting to observe the decreased auriophilic attraction in **1P** as a result of the protonation of the TPA ligand: the Au···Au separation at −80 °C increases by 0.21 Å upon ligand protonation. In the unprotonated bromide complex, **2**, the Au···Au separation is slightly longer at 298 K than the distance observed in the unprotonated chloride complex at −80 °C. This separation comes into agreement with the shortened Au···Au separation predicted by Pyykkö upon consideration of how the temperature (23 → −80 °C) affects the cell constants and the Au···Au separation (3.107 → 3.089 Å). The difference in the Au···Au separation in **1** and **2** shows that the effect is small, however, when Cl is replaced by Br. The large difference in the Au···Au separation between **1** and **1P** therefore is remarkable as is the effect of this increased Au···Au separation upon the solid state photoluminescence.

Compounds **1**, **1P**, and **2** are not luminescent in solution. Dilute solutions ($<10^{-5}$ M) of the complexes in MeOH glass also are not luminescent. The lowest absorption band of the complexes has been observed at an energy > 40 000 cm^{-1}, which is consistent with earlier studies[14] of linear tertiary phosphine Au complexes. The luminescence of mononuclear Au(I) phosphine complexes has been reported to show a dependence on the ligand concentration.[20] The low-energy photoluminescence properties observed in the complexes reported here are attributable to the Au···Au auriophilic attraction, which provides three-coordination in the solid state. In solution, where solvation competes with the auriophilic dimerization, intermolecular Au···Au interactions are minimal and emission is not observed.

It appears to be a general characteristic of the L–Au–X oligomers that pairs of molecules have the shortest metal–metal distances, while rings and chains have more, but longer Au···Au contacts. The Au···Au contact in **1** at −80 °C, 3.092(1) Å, is one of the shortest observed among the family of tertiary phosphines of Au(I) halides. Clearly, this is a consequence of lack of steric contact between phosphine ligands, a result arising from the small ligand cone angle, although a short Au···Au distance of 3.154(2) Å is also observed[27] in $Ph_3PAuSPh$, where the presence of the sulfur-bonded thiolate ligand presumably also contributes to the auriophilic bonding. Shorter contacts

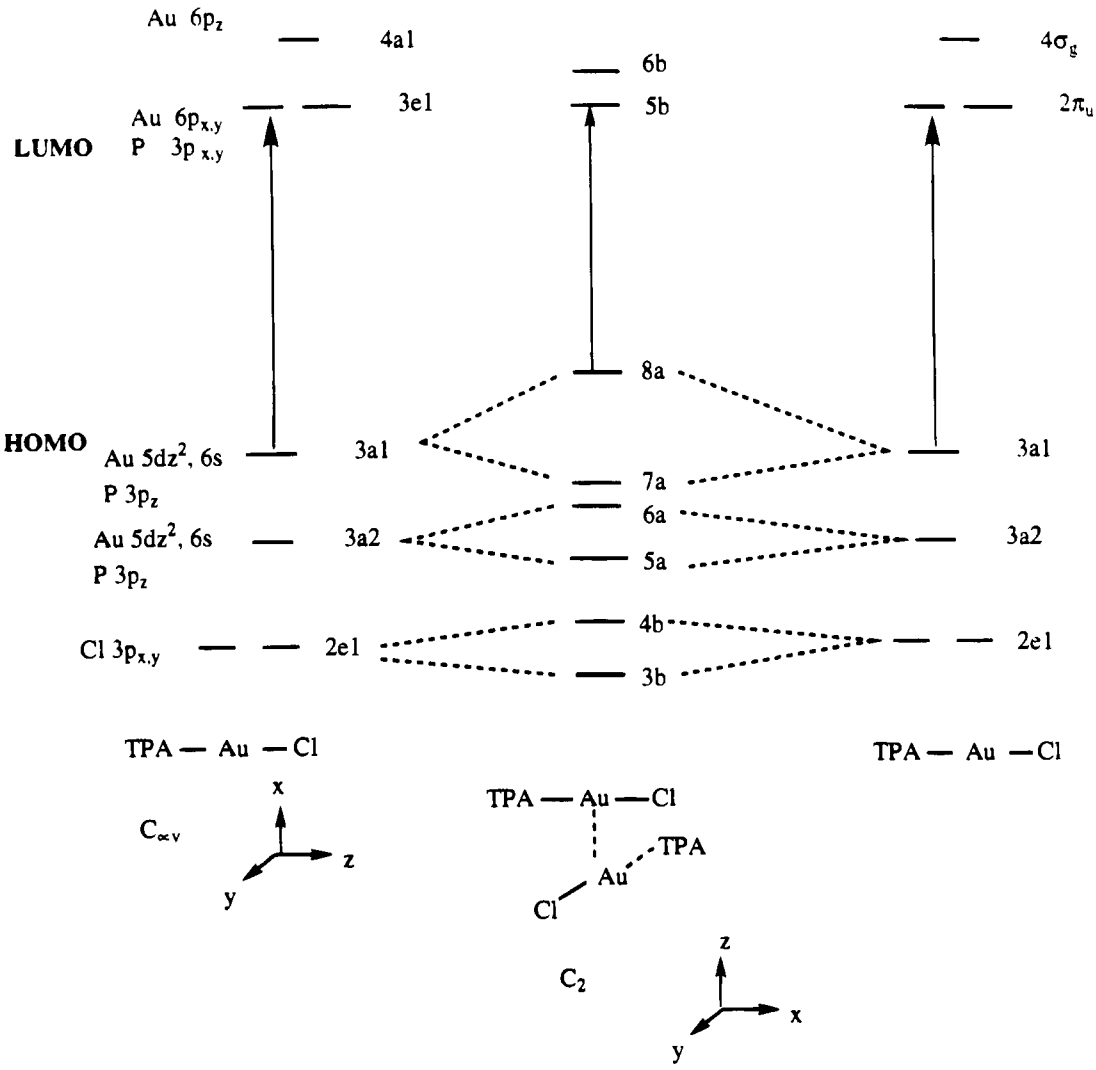

Figure 6. Extended Hückel molecular orbital diagram for the $[(TPA)AuCl]_2$ system. The calculation was performed on MM2-minimized structures using the CAChe program. The entire ligand is used in the calculation. The Au—P and Au—Cl distances were taken from the crystallographic data of **1**, and all other distances were used as found in the minimized structure. For the monomer the $C_{\infty v}$ point group is assumed. The z axis is defined as the molecular axis. For the dimer the Au—Au axis is defined as the z axis and the two molecules are perpendicular to each other. The MO diagram is given in the C_2 point group.

are found only in polynuclear complexes with bi- or polyfunctional ligands, where strain-free conformations and the "entropy-kick" favor the Au···Au interaction. It is not yet known what conditions favor polymeric forms over small oligomers (such as dimers). Since the energy associated with Au···Au interactions is small, even minor differences in lattice energies as derived from different crystal packing modes of the molecules can contribute significantly to the energy balance of each individual system.

Extended Hückel calculations indicate that when two isolated LAuCl units are brought together, the HOMO (σ_u orbital) is destabilized, Figure 6, and as a result the HOMO—LUMO gap decreases, Figure 7. Similar conclusions have been reached with previous work on $Au(CN)_2^-$ ions.[15] The short Au···Au separation in **1** is expected to destabilize the HOMO and thereby decrease the HOMO—LUMO gap. Compared to the case of **1P**, the red shift of the emission band of **1** reflects the increased Au···Au interaction found for this complex, and thus a reduced HOMO—LUMO gap. These extended Hückel calculations, which include a relativistic correction for Au, predict a shallow bonding minimum for a Au···Au separation of about 3.15 Å, Figure 8.

The blue shift observed in the emission bands of both **1** and **1P** with increasing temperature for 78 to 298 K also is consistent with an increased Au···Au separation as a result of thermal expansion. Accordingly, as the HOMO—LUMO gap increases, with increasing Au···Au distance, the luminescence band blue-shifts. The blue shift observed for **1P** between 78 and 250 K (about 700 cm^{-1}) compared with the blue shift for **1** (about 400 cm^{-1} between 78 and 250 K) apparently reflects the enhanced strength (less shallow potential well) of the shorter Au···Au bond in **1**. A second emission of a charge transfer origin is observed in the spectra of **2** and **3**. However, details of the comparative emission spectroscopies of **1—3** will be reported elsewhere.[28]

Similar to the situation observed for **1** and **1P**, a blue shift associated with a temperature increase also has been observed[15] in the solid emission spectra of $KAu(CN)_2$ and $TlAu(CN)_2$. The

(27) Fackler, J. P., Jr.; Staples, R. J.; Elduque, A.; Grant, T. *Acta Crystallogr.* **1994**, *C50*, 520. Nakamoto, M.; Hiller, W.; Schmidbaur, H. *Chem. Ber.* **1993**, *126*, 605.

(28) Assefa, Z.; McBurnett, G. B.; Staples, R. J.; Fackler, J. P., Jr. *Inorg. Chem.*, to be submitted for publication. Lifetime measurements were conducted at the Center for Fast Kinetics Research University of Texas at Austin, and will be presented in this paper.

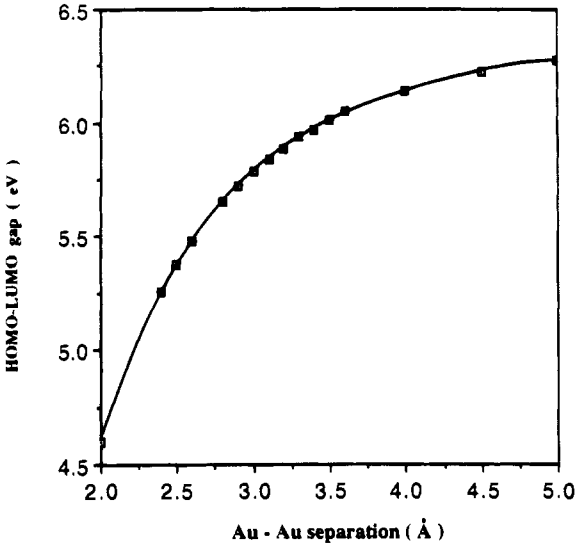

Figure 7. HOMO−LUMO gap vs Au−Au separation in the $[(TPA)AuCl]_2$ system. The entire ligand is used in the calculation. The Au−P and Au−Cl distances were taken from the crystallographic data. Other bond distances were used as found from the MM2-minimized structure. The z axis is defined as the Au−Au axis, and the two molecules are perpendicular to each other. The line was calculated using a polynomial to r^4, with coefficients of −7.0962, +11.521, −3.9062, +0.60679, and −3.5887 e^{-2} for r^0 to r^4, respectively.

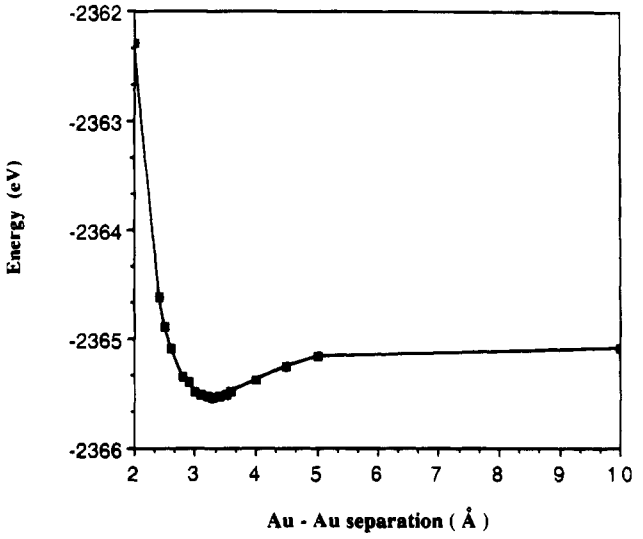

Figure 8. One-electron stabilization energy as a function of the Au−Au separation. The entire ligand is used in the calculation. The two molecules are perpendicular to each other with the Au−Au vector defined as the z axis. After minimization of the geometry, one of the molecules was kept at a fixed position and the other molecule was moved along the z axis. The EH calculation was conducted at various Au−Au distances.

$Pt(CN)_4^{2-}$ ion has no strong absorption bands below 35 000 cm^{-1} in solution, even though its salts are brightly colored and show strong visible luminescence in the solid state.[29]

Yersin and Gliemann have demonstrated[30] that the emission and reflectivity energies for nonbonded exciton complexes vary linearly with r^{-3} (where r is the metal−metal separation). This relationship between the intermolecular metal−metal distance and the emission energy has been used to explain the photophysical properties of several Au(I) complexes in the solid state.[31] We have attempted to correlate the emission properties of compounds **1** and **1P** with the Frenkel exciton model using eq 1,where E is the emission energy, E^0 is the energy of the

$$E = E^0 - a/r^3 \quad (1)$$

lowest absorption band corresponding to the isolated molecule, and r corresponds to the intermolecular Au···Au separation. The parameter α was estimated to be 7.8×10^5 from the spectroscopic and structural data for compound **1** (E = 674 nm, E^0 = 242 nm, r = 3.09 Å). By substituting the emission energy of **1P** at 298 K (584 nm), we calculated the Au···Au separation to be 3.22 Å, a result clearly too small compared with the observed distance of 3.31 Å.

Both chloride compounds reported here have a broad excitation band that extends from below 250 to 320 nm. The large Stokes shift between the excitation and emission bands suggests that the emission in both compounds is phosphorescence. The lifetime data are also consistent with this assignment.[31] The long lifetime observed for these complexes suggests that the emission originates from a spin-forbidden triplet state.

The HOMO−LUMO gap as calculated by the CAChe program (Figure 7) underestimates the observed change in the emission energy, E_n, with distance, assuming a spin-pairing energy, P, which remains constant at about 12 000 cm^{-1}. This energy difference corresponds to the 12 000 cm^{-1} separation between the $^1D_2$ and $^3D_2$ levels in the free Au^+ ion and is only 4200 cm^{-1} smaller than the separation between the singlet, $^1D_2$, state and the lowest energy triplet state in the free ion system.[32] However, the emission energy at 200 K using structural data at −80 °C for both **1** and **1P** does correlate reasonably well with an equation of type (2). Perhaps such a relationship can be

$$(E_1 + P)/r_1 = (E_2 + P)/r_2 \quad (2)$$

understood if it is assumed that the HOMO−LUMO energy ($E_n + P$) is linearly related to the overlap of the ground state and excited state wave functions in a weakly perturbed system. For example, the δ to δ^* transition in certain quadruply bonded systems having no lone pair electrons on the ligands shows such a behavior experimentally[33] and a long linear region of overlap exists theoretically.[34] In the system reported here, the HOMO−LUMO transition involves orbitals with substantial components perpendicular to the Au···Au axis, as suggested by the MO calculations, orbitals which overlap only weakly with each other at the distances observed. Is this linear behavior for the HOMO−LUMO separation energy not simply another characteristic to be expected of the weakness of the auriophilic bond between the two metal atoms?

Comparison of the solution absorption data of **1** and **1P** with those of other tertiary phosphine Au(I) complexes may help to understand the σ-donating ability of the sterically unconstrained TPA ligand. When compared to the lowest energy absorption bands of Me_3PAuCl and Et_3PAuCl (235 nm), the bands of **1** and **1P** (242 nm) are red-shifted by ca. 1400 cm^{-1}. A similar red shift in LAuX complexes has been suggested as an indication of an increased P-donor π-involvement in the LUMO orbital.[14a,b] Similarly, the red shift observed in the lowest absorption band of **1** and **1P**, when compared to Et_3PAuCl, indicates that the TPA ligand has a greater inductive σ-donor ability than the

(29) Jones, L. H. *J. Chem. Phys.* **1957**, *27*, 468.
(30) Yersin, H.; Gliemann, G. *Ann. N.Y. Acad. Sci.* **1978**, *313*, 539. (b) Yersin, H.; Gliemann, G.; Rossler, U. *Solid State Commun.* **1977**, *21*, 915.
(31) Fischer, P.; Ludi, A.; Patterson, H. H.; Hewat, A. W. *Inorg. Chem.* **1994**, *33*, 62.
(32) In Atomic Energy Levels. Circular 467; Moore, C. E., Ed.; U.S. Department of Commerce, National Bureau of Standards: Washington, DC, 1958; Vol. 3, p 190.
(33) Sattleberger, A. P.; Fackler, J. P. *J. Am. Chem. Soc.* **1977**, *99*, 1258.
(34) Trogler, W. K. *J. Chem. Educ.* **1980**, *57*, 424.

tertiary alkylphosphines, PEt_3 and PMe_3. Mason et al.[14] have shown that replacing the halide in LAuX by a phosphine to form L_2Au^+ complexes causes a red shift in the lowest absorption bands. For example, the lowest band of $(Et_3P_3)_2$-Au^+ (251 nm) is red-shifted by about 2400 cm^{-1} when compared to that of Et_3PAuCl or Me_3PAuCl (235 nm). The shift to lower energy again indicates an increased P-donor π-involvement in the LUMO of L_2Au^+ when compared to LAuX systems. Thus TPA behaves predominantly as a strong σ-donor.[2]

Upon protonation, the σ-donating ability of the TPA ligand might be expected to be reduced. The structural changes observed between **1** and **1P** which relate to the metal−ligand bonding are significant only in the gold−gold separation. The EH calculations conducted on the monomers, (TPA)AuCl and $[(TPAH)AuCl]^+$, suggest a reduced contribution of the ligand (mainly the C and N atoms) to the HOMO upon protonation. (All ligand atoms were included in the EH calculation and the parameters are given in Table 6.) The HOMO of the unprotonated (TPA)AuCl compound consists of 21.8% Au (7.1% 6s and 14.7% $5d_{z^2}$), 25.8% P ($3p_\sigma$), and 46.8% C, N ($2p_\sigma$). The metal contribution to the SHOMO is much larger (33%). The LUMO has a composition typical of a two-coordinate Au complex with a π-acceptor ligand with a 24.8% $3p_{\pi^*}$ and 40.7% $3d_{\pi^*}$ contributions from the P atom as well as 20% from Au $6p_{\pi^*}$ orbitals. Upon protonation, the metal $5d_{z^2}$ contribution to the HOMO increases (8.2% 6s and 19.3% $5d_{z^2}$) and the C, N p_σ contributions decreae (42.9%). The P $3p_\sigma$ contribution remains almost the same (25.7%) upon protonation. The increase in the gold−gold separation of the dimeric units upon protonation may reflect the decreased covalency of the metal−ligand system. However, intermolecular repulsion associated with the charge on the ligand also may be important to this distance change.

Conclusions

The remarkable shift in the emission spectrum of unprotonated and protonated (TPA)AuCl, **1** and **1P**, is attributed to the difference in the auriophilic Au···Au interactions observed in the solid state. There is a significant increase in the Au···Au separation as a result of protonation of one of the nitrogen atoms located three atoms away from the gold center. A consequence of the increased Au···Au separation is the observation that compound **1P** emits at a significantly blue-shifted position when compared to that of the unprotonated compound **1**. The emission energy of both the protonated and unprotonated complexes shows a temperature-dependent shift to higher energies with increasing temperature, consistent with the anticipated thermal expansion. EH calculations have indicated that the HOMO−LUMO gap in the complexes relates directly to the Au···Au separation. Due to the large separation between the excitation and emission bands, both the yellow emission of **1P** and the intense red emission of **1** are assigned as phosphorescence originating from the triplet state. In addition, several other derivatives of (TPA)AuX have been synthesized, including the organometallic species (TPA)AuMe.

Finally, it should be pointed out that the aggregation of Au(I) complexes through the extra forces originating from Au···Au contacts is emerging as another element for the design of *supramolecular frameworks*. It is a fortunate coincidence that these forces are similar in energy to those of hydrogen bonds, which to date provide the most useful binding motifs for supramolecular aggregates. At the present stage of knowledge, H-bonds are more dependable regarding the number and orientation of their interactions. However, as the number of well-characterized examples of Au···Au interactions becomes larger, the concept of "auriophilicity" is expected to grow into a constructive pattern of structure and reactivity features.

Acknowledgment. In the U.S.A., the support of the National Science Foundation (Grant CHE-9300107), the Robert A. Welch Foundation, and the Texas Advanced Research Program is gratefully acknowledged. In Germany, the study was supported by the Deutsche Forschungsgemeinschaft and the Fonds der Chemischen Industrie. The authors are particularly grateful to the Pinguin Foundation for continued support under the Manchot Research Professorship (J.P.F.) since 1992.

Supplementary Material Available: Tables of H atom positions and anisotropic temperature coefficients for each structure (3 pages). Ordering information is given on any current masthead page.

IC9406749